# A THERMODYNAMIC MODEL TO QUANTIFY THE IMPACT OF COOLING IMPROVEMENTS ON GAS TURBINE EFFICIENCY

**Selcuk Can Uysal***
National Energy Technology Laboratories
Morgantown, WV, USA

**Eric Liese**
National Energy Technology Laboratories
Morgantown, WV, USA

**Andrew C. Nix**
West Virginia University
Morgantown, WV, USA

**James Black**
National Energy Technology Laboratories
Pittsburgh, PA, USA

## ABSTRACT

Cooling of turbine hot-gas-path components can increase engine efficiency, reduce emissions, and extend engine life. As cooling technologies evolved, numerous blade cooling geometries have been, and continue to be proposed by researchers and engine builders for internal and external blade and vane cooling. However, the impact of these improved cooling configurations on overall engine performance is the ultimate metric. There is no assurance that obtaining higher cooling performance for an individual cooling technique will result in better turbine performance because of the introduction of additional second law losses, e.g. exergy loss from blade heat transfer, cooling air friction losses, fluid mixing, etc. and thus the higher cooling performance might not always be the best solution to improve efficiency.

To quantify the effect of different internal and external blade cooling techniques and their combinations on engine performance, a cooled engine model has been developed for industrial gas turbines and aero-engines using MATLAB Simulink®. The model has the flexibility to be used for both engine types, and consists of uncooled on-design, turbomachinery design and a cooled off-design analysis in order to evaluate the engine performance parameters by using operating conditions, polytropic efficiencies, material information and cooling system information. The cooling analysis algorithm involves a Second Law analysis to calculate losses from the cooling technique applied.

The effects of variations in engine parameters such as turbine inlet temperature, by-pass ratio, and operating temperature are studied. The impact of variations in metal Biot number, thermal barrier coating Biot number, film cooling effectiveness, internal cooling effectiveness and maximum allowable blade temperature on eng[1]ine performance parameters are analyzed. Possible design recommendations based on these variations, and direction of use of this tool for new cooling design validation, are presented.

## 1. INTRODUCTION

The ultimate goal in engine design is to produce the highest available power or thrust at the maximum efficiency with minimal fuel consumption and emissions. Turbine blade cooling increases the performance of both aero-engines and industrial gas turbines through higher allowable combustor exit temperatures and providing longer engine life. Numerous cooling techniques have been and continue to be developed by researchers and engine producers for internal and external disk and blade cooling.

There are a wide variety of cooling techniques that have been applied to certain engine designs. This required the need of assessing the relative benefits of a certain cooling technique compared to other techniques from an overall engine performance perspective. To accomplish this, a thorough thermodynamic model of the gas turbine including the turbine cooling effects needs to be used.

Several researchers have developed thermodynamic models for cooled turbine analysis. One of the most detailed models is by Consonni [1]; with other prominent ones such as GASCAN by El-Marsi [2], CPF by NASA [3], TURBOMATCH by Lallini

*This work was done under the U.S. Department of Energy (DoE) Graduate Research Program at the National Energy Technology Laboratory (NETL), managed by the Oak Ridge Institute for Science and Education (ORISE)

et al. [4] and IGCC by Li et al. [5]. The latter two models have a typical aero-engine or industrial gas turbine cycle calculation coupled with a cooled turbine model. TURBOMATCH [4] differs by also including a turbomachinery algorithm. In general, cooled turbine analysis models contain a coolant fraction calculation sub-routine followed by a 1st Law Analysis. This 1st Law Analysis involves a continuity and energy balance for each stage component. The analysis is then completed with estimations of cooling related losses (e.g. exergy loss from blade heat transfer, cooling air friction losses, fluid mixing, etc.) through a pressure loss correlation term [6], or in advanced models with a detailed 2nd Law Analysis, which involves the calculation of entropy generation through a relevant heat transfer and momentum analysis.

A detailed analysis of a cooled turbine involving the 2nd Law losses was proposed by Young et al. [7], which also includes rotational effects and stage loading information in rotor equations. In the current study, the methodology and approach by Young et al. [7] is used to develop a cooled turbine model, and this model is later integrated into an engine performance estimation model by Uysal [11], to quantify the effects of improvements in various cooling techniques on overall engine performance. The models developed in the current work are unique in reducing the number of inputs required to perform the analysis of cooling technology impact on overall engine performance parameters, and provides the flexibility to input experimental or computational fluid dynamics (CFD) data obtained for a certain cooling design.

## 2. THEORY

The cooled turbine stage considered in this analysis is assumed to be formed by the following components: a purge before stator, a stator stage, another purge between the stator and rotor and the rotor stage. Figure 1 shows this sequence with mainstream and coolant flow notations.

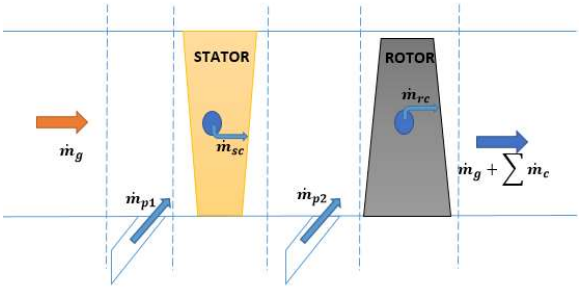


**Figure 1. Cooled turbine stage components used in the model shown with hot and cold side gas flows**

The stator and rotor cooling flows include the coolant flows injected into mainstream by all means of external cooling techniques, i.e. film cooling, trailing edge cooling, tip cooling etc. The model uses a semi-empirical approach to calculate the required coolant flows by using the formula given in Equation (1) for a cooled blade having both internal and external cooling with a thermal barrier coating (TBC) layer [8, 9].

$$\frac{\dot{m}_c}{\dot{m}_g} = \frac{K_{cool}}{(1 + Bi_{total})}\left\{\frac{\varepsilon_0 - \eta_{fc}(1 - \eta_c(1 - \varepsilon_0))}{\eta_c(1 - \varepsilon_0)}\right\} \quad (1)$$

In Equation (1), $Bi_{total}$ is the total Biot number calculated for the metal and TBC materials, $\varepsilon_0$ is the overall cooling effectiveness for the blade, $\eta_{fc}$ is the film cooling effectiveness, and $\eta_c$ is an internal cooling effectiveness. $K_{cool}$ is a parameter given by Young et al. [7] as well but modified here to include internal and external Stanton numbers, as well as the flow-turning angle across the stage, and the solidity of the cooled blade [10] which provides more information on the blade passage geometry to the calculations. If one of the considered cooling techniques is not present in the stage, then Equation (1) can still be used by eliminating the relevant efficiency or Biot number.

Enthalpy values at each stage component are needed to obtain thermodynamic properties at each cooled turbine component. The derivations for these were made with energy and continuity balances written for each stage component. The derivation of enthalpy equations for the purge/disk cooling and stator comes from basic mixing flow analysis of two streams (hot gas and the coolant) and are given in Equation (2a) and (2b), respectively [7]. The rotor enthalpy equation, given in Equation (2c), is derived from the rothalpy balance and relative to static enthalpy transformations. Swirl effects are included in the calculations through a constant parameter ($K_{swirl}$) and power generated in the rotor stage is included with the stage loading parameter ($\psi$).

$$h_{t,p1} = \frac{(\dot{m}_g)h_{t,g} + \dot{m}_p h_{t,pc}}{(\dot{m}_g + \dot{m}_p)} \quad (2a)$$

$$h_{t,s} = \frac{(\dot{m}_g + \dot{m}_p)h_{t,p1} + \dot{m}_{sc}h_{t,sc}}{\dot{m}_g + \dot{m}_{sc} + \dot{m}_p} \quad (2b)$$

$$h_{t,r} \cong \frac{h_{t,rc} - \frac{(K_{swirl} - 0.5)}{\psi}\left(h_{t,p2} + \frac{\dot{m}_{rc}}{\dot{m}_g + \dot{m}_{sc} + \dot{m}_p}h_{tr,c}\right)}{1 - \frac{(K_{swirl} - 0.5)}{\psi}\left(1 + \frac{\dot{m}_{rc}}{\dot{m}_g + \dot{m}_{sc} + \dot{m}_p}\right)} \quad (2c)$$

Calculating the entropy generation across the cooled turbine stage ($\dot{\sigma}_{stage}$) completes the cooled turbine analysis. This information can then either be used to calculate exergy from $-T_0\dot{\sigma}_{stage}$ to calculate the loss in turbine work due to cooling, or can be used in computing the cooled turbine pressure ratio that is an engine performance parameter. For each turbine stage station (i.e. purge, stator, or rotor) the entropy rise and the pressure ratio of the turbine station can be related by using Equation (3), from the 2nd Law of Thermodynamics.

$$\dot{\sigma}_{station} = s^0(T_{station.ext}) - s^0(T_{station.in}) - Rln\left(\frac{P_{station.ext}}{P_{station.in}}\right) \quad (3)$$

In Equation (3), $s^0(T)$ indicates the entropy rise from absolute zero to the temperature T, which can be calculated using reduced pressures that is usually tabulated for most of the working fluids used in gas turbines [12].

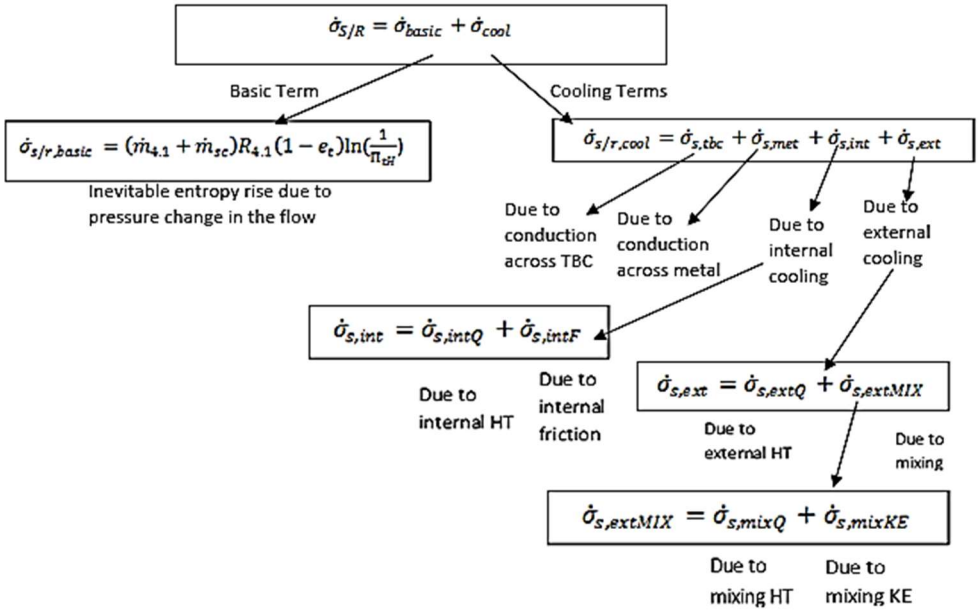


**Figure 2. Schematic of the model for entropy generation calculations from Young et al. [7]**

Overall stage pressure ratio can be found by multiplying the station pressure ratios that are obtained by using Equation (3) for each subsequent turbine component. After re-arranging, overall entropy generated in the cooled turbine stage can be found as a linear combination of entropies generated at each stage component, as given in Equation (4).

$$\dot{\sigma}_{stage} = \dot{\sigma}_{purge} + \dot{\sigma}_{rotor} + \dot{\sigma}_{stator} \qquad (4)$$

The purge cooling term in Equation (4) can be obtained from a mixing analysis of two flows. However, for the stators and rotors cooling losses should be calculated with an advanced model that includes all possible cooling losses introduced in these components. Such a model was introduced by Young et al. [7], which is schematized in Figure 2, and can be used in the cooled turbine calculations conveniently.

The assumed 1D heat transfer model used for the cooled blade and the associated entropy terms from [7] are shown in Figure 3.

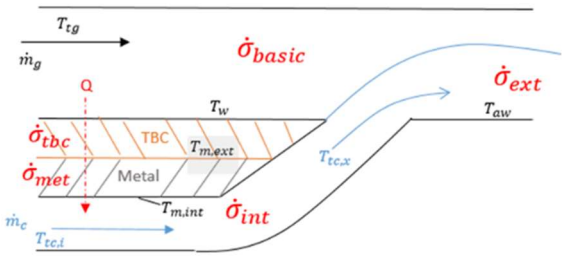


**Figure 3. The heat transfer model used in this study shown with associated entropy terms for a blade having internal and external cooling (film cooling) with a TBC layer**

Equations and derivations with assumptions to compute each of the entropy terms shown in Figure 2, are given in detail by Young et al. [7].

## 3. COOLED TURBINE MODEL

Based on the presented theory, a Cooled Turbine Model (CTM) is developed. The model consists of three main sub-systems: a coolant calculator for coolant fraction calculations based on the semi-empirical approach in Equation (1), an enthalpy calculation sub-system (1st Law Analysis) that calculates the component enthalpies from Equation (2) by using the coolant fractions calculated by the coolant calculator, and an entropy calculation sub-system (2nd Law Analysis) that employs the method by Young et al. [7] to calculate the associated cooling losses. The developed algorithm, that makes use of the discussed cooled turbine theory to calculate the engine performance variables, is shown in Figure 4.

The defined algorithm was modelled in MATLAB/Simulink® in order to use it within the Engine Design Model (EDM) developed by Uysal [11]. The EDM is an aerothermal engine performance calculation model that includes on-design, off-design, and a turbomachinery design sections for high by-pass turbofan engines. The model is based on the theory given by Mattingly et al. [12], which is based on the conservation of continuity and energy of the flow across the gas turbine components. The model assumes a steady-state quasi-1D flow with variable specific heat, and uses mean-line calculations with free vortex design in the turbomachinery section. Polytropic efficiencies include the effects of pressure and aerodynamic losses in compressor and turbine sections. Further details on the development and the theory behind the EDM can be found in the

study by Uysal [11], and will not be reproduced here. The EDM was validated both with AEDSys Software [12] and published engine data for CFM-56 and GE90 engines.

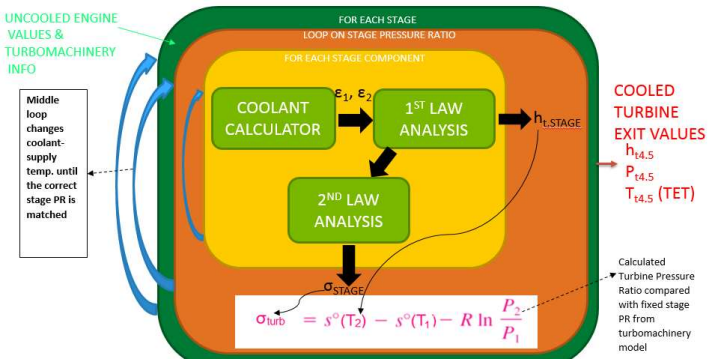


**Figure 4. Cooling Analysis Model Flowchart including the sub-models**

The CTM was verified with the example case results from Young et al. [7] for a single staged turbine using pure air in both hot gas and coolant sides. Mass flowrates and component exit total temperatures were the main parameters shown in the comparison in Table 1.

**Table 1. Validation of the coolant calculator and 1st Law analysis results are done with the Young et al. [7]**

| Parameter | CTM | Young et al. [7] | %Difference |
|---|---|---|---|
| *Stator* | | | |
| Cooling Fraction | 0.145 | 0.145 | 0.0% |
| Exit Total Temperature (K) | 1598 | 1603 | 0.32% |
| *Rotor* | | | |
| Cooling Fraction | 0.050 | 0.049 | 2.04% |
| Exit Total Temperature (K) | 1484 | 1487 | 0.21% |

Small discrepancies in the comparison are likely due to the use of different thermodynamic property tables.

For the same example case, the results of the 2nd Law analysis were also given by Young et al. [7] for individual entropy terms. By using this information, a comparison of the results of 2nd Law analysis was also made and is shown for a stator stage in Figure 5.

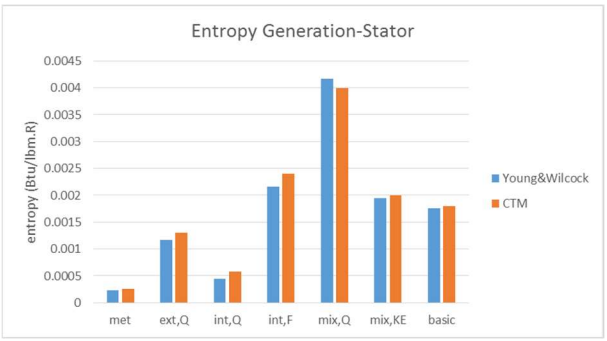


**Figure 5. Stator entropy rise calculated for each source term and compared with Young et al .[7]**

The differences in results were within the range of error associated from plot digitizing of the data from [7], and variations in thermodynamic property tables.

## 4. COOLED ENGINE MODELS

Cooled Engine Models are developed in MATLAB Simulink® to perform the cycle calculations that will calculate engine performance parameters. These models are developed for a turbofan (aero-engine) case and for an industrial gas turbine case and named as Cooled Engine Design Model (CEDM) and Cooled Gas Turbine Model (CGTM), respectively. Both models are based on the Engine Design Model (EDM) developed and validated by Uysal [11] for a high by-pass turbofan engine.

EDM, the basis engine model for development, is an engine design and performance calculation model, which also has an aerothermal turbomachinery design section and is based on the theory given by Mattingly et al. [12]. In this model, turbine cooling was included in calculations through the usage of two "coolant mixer" stations; the first one is before the high pressure turbine and the second one is after the high pressure turbine and before the first stator vane of the low pressure turbine. In the cooled engine models, these stations are removed and cooled turbine stage exit properties are calculated in a separate sub-system, which has the cooled turbine model (CTM) algorithm. Extending the capabilities of EDM through the addition of the cooling model also allows calculation of the cooling related heat transfer and pressure losses, instead of using a lumped polytopic efficiency to reflect the influence of these effects on the component performance.

Cooled turbine calculations require parameters from the uncooled engine cycle calculations and turbomachinery design. To obtain this information, the on-design and turbomachinery design sections of EDM are retained in the cooled engine models. A schematic of the cooled engine models with their major sub-systems is shown in Figure 6.

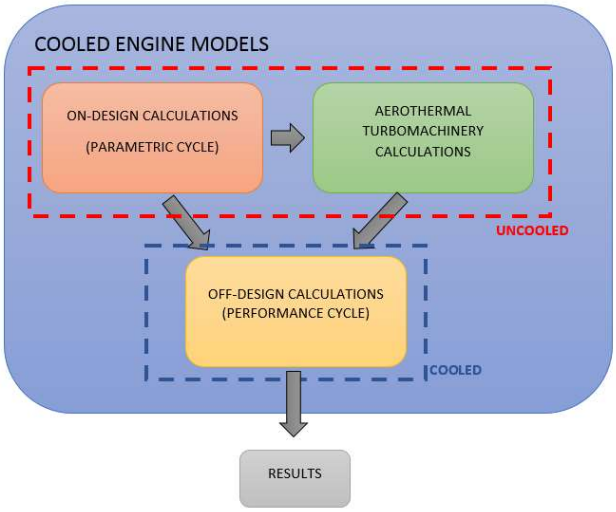


**Figure 6. Flowchart for the cooled engine models**

In the cooled engine models, the cooled engine performance is treated as an off-design point, that is, a performance cycle modelling approach is used. The flowchart of the cooled off-design section of CEDM is given in Figure 7. The same flowchart is also valid for CGTM, except the low pressure spool components, fan and secondary exhaust sections. For CGTM case, turbine represents a power turbine and the exhaust nozzle is replaced by a diffuser that applies the defined back-pressure ratio.

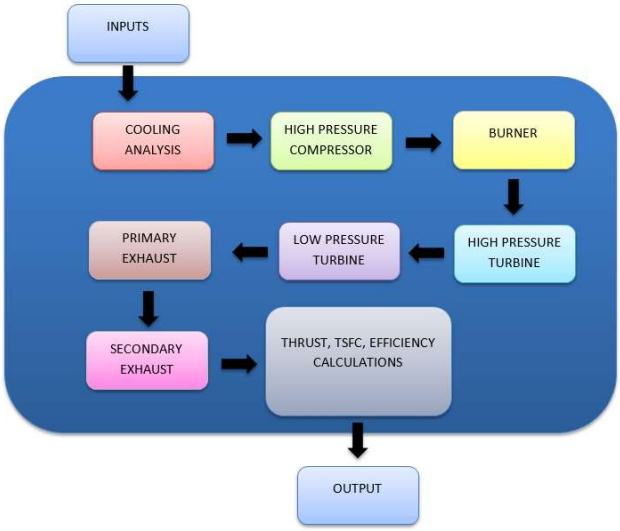


**Figure 7. Flowchart of the cooled off-design section**

The cooled off-design section starts calculations with a cooling analysis sub-model, which uses uncooled engine compressor supply pressures and temperatures to calculate the coolant fractions in the cooled engine. These fractions are then later used in the high pressure compressor sub-system to include the effect of coolant extraction on compressor performance. This effect is calculated by dividing the compressor of the cooled engine into multiple small compressors operating with different air flowrates calculated by subtracting the turbine coolant flows (includes purge flows). Determination of coolant extraction stages from the compressor is achieved within the cooling analysis section automatically, by using the turbomachinery section results for stage pressures of each rotating component. The high pressure turbine sub-system uses coolant fractions together with entropy rise calculated at the cooling analysis section to calculate the cooled turbine performance parameters (pressure ratio, temperature ratio, isentropic efficiencies, etc.).

Relating the entropy rise to physical engine quantities is made possible through the 2nd Law of Thermodynamics defined for the entire turbine. Re-arranging the 2nd Law with variable specific heats will then yield the relation used to calculate cooled turbine pressure ratio as given in Equation (5).

$$\pi_{tH,cooled} = e^{-\frac{(\dot{\sigma}_{turb}-(s^0(T_{turb,exit})-s^0(T_{turb,inlet})))}{R_{avg}}} \quad (5)$$

In this Equation (5), $R_{avg}$ is the average real gas constant between the cooled turbine inlet and exit states.

Validation of the CEDM was carried out for a CFM56-5A high by-pass turbofan engine with available published engine data [14]. The comparison of published engine data with CEDM results is documented in Table 2.

**Table 2. Validation of the CEDM with published engine data for CFM56-5A Engine [14]**

| Parameter | CEDM | Engine Data [14] | %Difference |
|---|---|---|---|
| Thrust (lbf) | 23506 | 23700 | 0.82% |
| Fuel Consumption (lbm/hr) | 0.6089 | 0.5967 | 2.04% |
| Exhaust Gas Temperature (°C) | 861 | 855 | 0.70% |

In the comparison case of Table 2, internal cooling, film cooling, and TBC layer are all assumed to be used in the high pressures stages of the turbine. Variations in results are a result of different purge flow fractions, cooling technology parameters and fan and exhaust losses.

Further validation was carried out for individual component performance parameters such as isentropic efficiencies, temperature ratios and pressure ratios. Validation was accomplished by comparing the results of CEDM with GasTurb12 [13] for an aero-engine with an input set given in Appendix-A. In order to make both models comparable, calculated coolant fractions from CEDM (9.46% of the core flow, including purge flows) were also used as an input to GasTurb12. The comparison is shown in Table 3.

Use of additional pressure loss correlations [13] in the fan and exhaust sections by GasTurb12 is a possible explanation for slightly lower temperature and pressure ratios. Using different cooled turbine models also results in differences in turbine exit temperatures and lower temperature ratios in CEDM calculations. However, for all compared parameters the differences are within reasonable limits (less than 3%).

**Table 3. Result comparison of CEDM with GasTurb12 for the same turbofan engine input set**

| Parameter | GasTurb12 | CEDM |
|---|---|---|
| $\pi_r$ | 1.53 | 1.53 |
| $\tau_d$ | 1 | 1 |
| $\eta_f$ | 0.93 | 0.93 |
| $\tau_f$ | 1.1 | 1.14 |
| $\eta_{cL}$ | 0.90 | 0.90 |
| $\tau_{cL}$ | 1.15 | 1.15 |
| $\eta_{cH}$ | 0.84 | 0.84 |
| $\tau_{cH}$ | 2.44 | 2.49 |
| $f$ | 0.025 | 0.025 |
| $\eta_{tH}$ | 0.94 | 0.94 |
| $\tau_{tH}$ | 0.74 | 0.73 |
| $\pi_{tH}$ | 0.26 | 0.27 |
| $\eta_{tL}$ | 0.94 | 0.94 |
| $\pi_{tL}$ | 0.37 | 0.38 |
| $\tau_{tL}$ | 0.81 | 0.79 |
| $P_{t9}/P_0$ | 3.85 | 3.87 |
| $T_{t9}$ (°R) | 1670 | 1676 |
| $P_{t18}/P_0$ | 2.32 | 2.32 |
| $\eta_p$ | 0.73 | 0.73 |

The effect of cooling the turbine on overall engine performance parameters can be demonstrated by comparing the uncooled and cooled version of the same engine. This comparison is shown for the input case used in the previous comparison in Table 4.

**Table 4. The effect of cooling on turbofan engine parameters**

| Parameter | Uncooled | Cooled | %Difference |
|---|---|---|---|
| $f$ | 0.0249 | 0.0248 | -0.4% |
| $\eta_{tH}$ | 0.9408 | 0.9412 | +0.04% |
| $\tau_{tH}$ | 0.7491 | 0.7318 | -2.31% |
| $\pi_{tH}$ | 0.282 | 0.27 | -6.38% |
| $\eta_{tL}$ | 0.9388 | 0.9391 | +0.03% |
| $\pi_{tL}$ | 0.4008 | 0.3802 | -5.14% |
| $\tau_{tL}$ | 0.7982 | 0.7869 | -1.42% |
| $T_{t9}$ (°R) | 1739 | 1676 | -3.62% |
| Thrust (lbf) | 15268 | 14765 | -3.29% |
| TSFC (lbf/(lbm.hr) | 0.6916 | 0.6674 | -3.50% |
| $\eta_p$ | 0.7263 | 0.7334 | +0.71% |

When turbine cooling is present, the effect of coolant extraction from the compressor reduces the air flowrate to the burner, which reduces the fuel to air ratio by a small fraction (0.4%). Due to increased entropy at the turbine due to cooling, the primary effect on high pressure turbine physical parameters is a reduction in turbine pressure ratio (6.4%). However, reducing the turbine exit temperature to a lower temperature than the uncooled turbine results in an increase in isentropic turbine efficiency (0.04%) and a reduction in turbine temperature ratio (2.3%). Low pressure turbine performance is also affected by the cooling of the high pressure turbine; due to a reduced inlet temperature and lower inlet pressure. With constant polytropic efficiency, in order to supply the constant amount of work to the fan and low pressure compressor, the low pressure turbine has a reduced exit pressure and this results in a reduction in low pressure turbine pressure (5%) and temperature ratio (1%). The overall effect was a 4% reduction in primary exhaust temperature. However, for fixed exhaust nozzle angle, reducing the exit pressure results in a reduction in thrust (3%), whereas increased turbine efficiencies result in an increase in propulsive efficiency (0.7%). Reduction in the fuel consumption was also noted for the engine case considered, but this effect might be case dependent as also noted by Esgar et al. [15].

In order to observe the differences in the cooled engine performance prediction by CEDM and GasTurb12 over a range of input parameters, flight Mach Number, engine by-pass ratio and turbine inlet temperature inputs were changed within a pre-determined range and the predictions of turbofan engine performance parameters were compared.

In a turbofan engine design given a fixed fan pressure ratio, increasing the engine by-pass ratio reduces the fuel consumption due to reduction in the core air flowrate [12]. This well-known effect is used as the first comparison case and the results obtained from CEDM and GasTurb12 is compared in Figure 8 while varying the by-pass ratio from 4 to 8. The differences between the results are within 3% throughout the input range.

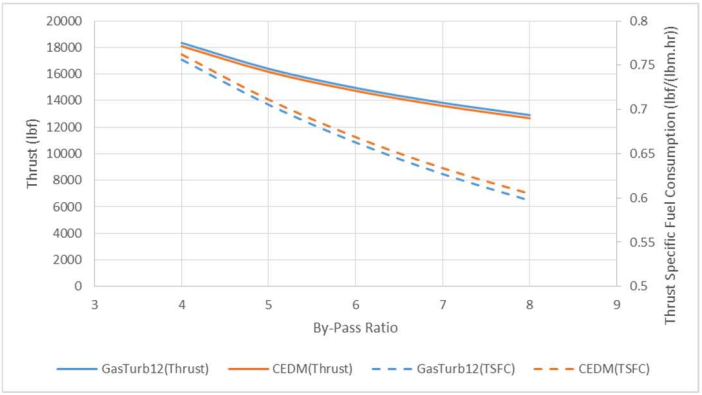


**Figure 8. The effect of changing engine by-pass ratio is compared for thrust and thrust specific fuel consumption**

Figure 9 shows the comparison made for an increase in turbine inlet temperature from 2469 °R to 3669 °R. The maximum difference between the predictions by CEDM and GasTurb12 in Figure 9 is within 3%. As the turbine inlet temperature is increased, due to the increase in required turbine cooling flows, the thrust curve slope is less positive after ~2750 °R because of increased turbine losses and compressor work. Reduction rate in propulsive efficiency also increased after this

temperature value. In turbofan engine design, this point corresponds to an optimum design point.

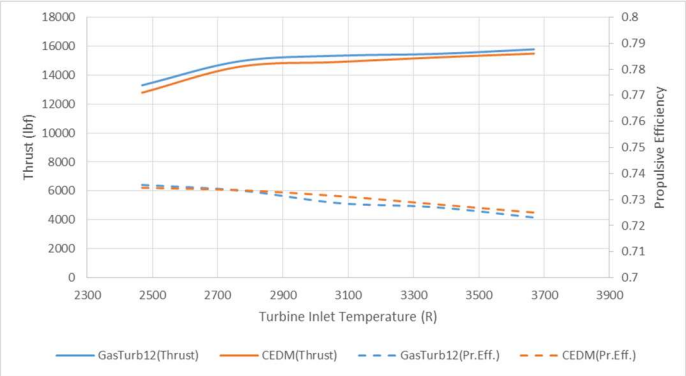


**Figure 9. The effect of changing the turbine inlet temperature is compared for thrust and propulsive efficiency**

Modification of EDM to CEDM required only the addition of the cooled off-design section. CGTM development, however, required several additional considerations. Aside from removing turbofan related engine components, this development process included the following: an adjustment of the cycle calculations of turbine and exhaust sections for a land based engine, changing performance parameter definitions, usage of natural gas fuel combustion tables instead of kerosene, adding a transition cooling model and modification of the turbomachinery design section per industrial gas turbine design principles.

According to Soares [16], industrial gas turbines are similar to turbojet aero-engines, in which zero thrust is produced. Therefore, the turbojet relations given by Mattingly et al. [12] are used by equating the thrust equation to zero. Resulting cycle analysis required the back-pressure ratio ($P_{t9}/P_{t0}$) to be a user input, which is the case in all industrial gas turbine simulations. The transition cooling between the combustor and the turbine is modelled as a constant pressure mixer that mixes the hot gas from the combustor with the coolant extracted from the last stage of the compressor and calculates the regarding enthalpy change.

The CGTM uses a variable specific heat model for the air and combustion products. Therefore, thermodynamic property tables of fuel combustion products are used throughout the model to extract required thermodynamic properties (reduced pressure, temperature, enthalpy, and entropy) once the fuel to air ratio and a secondary thermodynamic parameter (temperature, enthalpy, reduced pressure or entropy) at that location is known. Values are tabulated for pure air and several pre-determined fuel to air ratios. For turbofan engines, these tables were for kerosene-air combustion [11, 12], which may cause additional errors up to 8% for each engine component if they are used in an engine using natural gas as a fuel [17].

In order to eliminate this potential error source, thermodynamic property tables for natural gas combustion (assumed 100% methane) was generated with a complete methane combustion reaction for four different fuel-to-air ratio conditions. GASEQ Software [19] was used to obtain molar fractions of the combustion products, and REFPROP Software [18] was used to generate thermodynamic tables. Obtained results were compared with the validation data by Guha [20] given for the calculated enthalpy differences between two specified temperatures for different fuel-to-air ratios for low and high temperature ranges. The comparison showed agreement with the compared data, and is given in Appendix-B.

The parameters in the turbomachinery design section of the CEDM model (based on a turbofan engine) for application to the CGTM model (based on an industrial engine), as described by Giampoulo [21], include: slower shaft speeds (i.e. lower rpm), lower internal flow speeds, lower compressor pressure ratios, lower aspect ratio in turbine blades, constant disk diameter, and longer blades. Calculations based on Mattingly et al. [12] in the CEDM were modified with the design equations from Wilson et al. [22] to obtain the design in the CGTM. The methodology used in aircraft engines was also modified here to make a constant rotational shaft speed design. Aside from usage of different materials, it was also found that the disk shape factors, compressor loss factors, and turbine stage loadings can be lower in industrial gas turbines than typical values used for aero-engines.

A validation (not shown) was carried out for the CGTM with available H-Class industrial gas turbine data by using blade heights, number of stages, and disk dimensions as the comparison parameters.

The results of the CGTM overall engine performance parameters such as shaft power delivered, heat rate, and thermal efficiency were compared with selected published H-Class industrial gas turbine data in Table 5. Input information on cycle inputs such as compressor pressure ratio, turbine inlet temperature, engine mass flowrate and ambient conditions were taken from the published values in [24].

**Table 5. Validation of CGTM outputs with published engine data**

| Parameter | CGTM | Published Value [24] |
|---|---|---|
| *Siemens SGT6-8000H* | | |
| Power (MW) | 296 | 296 |
| Thermal Efficiency (GT) | 40.0% | 40.0% |
| Heat Rate (Btu/kW.h) | 8526 | 8530 |
| Exhaust Temperature ($^0$F) | 1159 | 1160 |
| *General Electric GE7HA.02* | | |
| Power (MW) | 347 | 346 |
| Thermal Efficiency (GT) | 42.2% | 42.2% |
| Heat Rate (Btu/kW.h) | 8084 | 8080 |
| Exhaust Temperature ($^0$F) | 1153 | 1153 |
| *Mitsubishi-Hitachi Industries M501J* | | |
| Power (MW) | 327 | 327 |
| Thermal Efficiency (GT) | 41.0% | 41.0% |
| Heat Rate (Btu/kW.h) | 8325 | 8325 |
| Exhaust Temperature ($^0$F) | 1178 | 1176 |

A case specific comparison was carried out for the CGTM by using the same approach used for CEDM. The results obtained by CGTM and GasTurb12 for the same input set (given in Appendix-A) generated for an average H-Class industrial gas turbine case are shown in Table 6.

In the industrial gas turbine case, the differences between the results obtained by the CGTM and GasTurb12 for the component performance parameters are lower, mainly due to fewer engine components that have specific pressure or temperature loss models used in GasTurb12.

Similar to the continuity tests carried out for the CEDM, selected cycle input parameters such as turbine inlet temperature, ambient temperature and back pressure ratio were changed within a pre-determined interval and the trends obtained by the CGTM were compared with GasTurb12.

**Table 6. Result comparison of CGTM with GasTurb12 for the same industrial gas turbine input set**

| Parameter | GasTurb12 | CEDM |
|---|---|---|
| $\pi_r$ | 1 | 1 |
| $\tau_d$ | 1 | 1 |
| $\eta_c$ | 0.87 | 0.87 |
| $\tau_c$ | 2.60 | 2.67 |
| $f$ | 0.029 | 0.029 |
| $\eta_t$ | 0.94 | 0.94 |
| $\tau_t$ | 0.50 | 0.49 |
| $\pi_t$ | 0.050 | 0.049 |
| $P_{t9}/P_0$ | 1.03 | 1.04 |
| $T_{t9}$ ($^\circ$R) | 1613 | 1597 |
| HR (Btu/kWh) | 8241 | 8201 |
| $\eta_{th}$ | 0.416 | 0.416 |

Increasing the turbine inlet temperature has a well-known enhancing effect on the shaft power delivered and thermal efficiency. Due to increased combustor exit temperature, this increase will also reduce the overall fuel consumption. However, due to the increased coolant requirements to cool the turbine blades to a fixed lower temperature (fixed by the blade material used) the performance curves will have an optimum point as also observed in the turbofan engine case. Figure 10 shows the comparison made for thermal efficiency and power specific fuel consumption when the turbine inlet temperature is increased from 2660 $^\circ$R to 3460 $^\circ$R.

Similar to turbofan engine case, there exists an optimum point around a certain turbine inlet temperature (~3050 $^\circ$R), which was predicted the same by both the CGTM and GasTurb12. Above this optimum point, the advantages obtained from increasing the turbine inlet temperature are offset by the increased turbine losses and result in a reduction in engine performance.

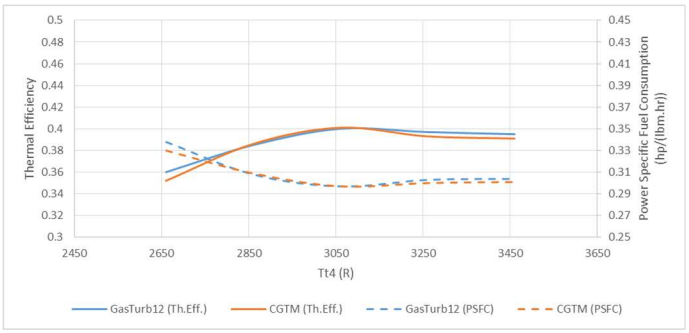


**Figure 10. The effect of changing the turbine inlet temperature is compared for thermal efficiency and power specific fuel consumption**

Another test was made by increasing the ambient temperature (while keeping turbine inlet temperature, and component efficiencies constant), which has an expected effect of reducing engine performance. This is due to the nature of the Brayton Cycle; increasing the engine inlet temperature will result in an increase in required compressor work, while the turbine is operating between the same pressure difference. In addition, increased coolant supply temperatures from the compressor will also reduce cooling performance in the turbine and results in a decrease in turbine performance as well. Figure 11 shows the comparison made for this test case, and the differences between the results obtained from CGTM and GasTurb12 are within 2%.

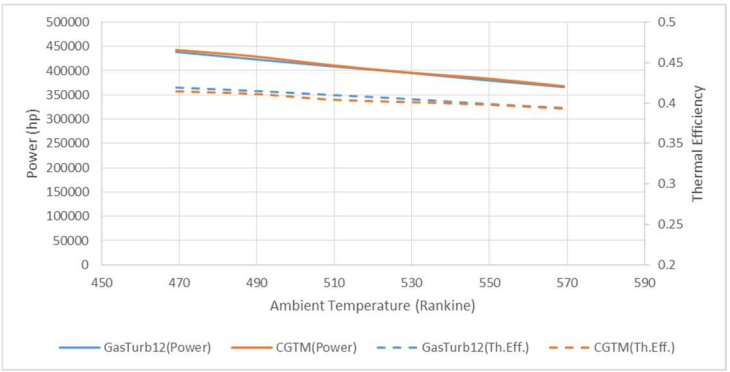


**Figure 11. The effect of changing the ambient temperature is compared for shaft power delivered and thermal efficiency**

## 5. SENSITIVITY ANALYSIS ON COOLING PARAMETERS

The sensitivity of selected cooling performance parameters was sought by comparing a percent change from the reference generic H-Class engine performance (Table 7). The reference values of Table 7 were determined from the values given by Wilcock et al. [23] for "advanced cooling technology" levels, which is a viable assumption for recent H-Class engine technology. Sensitivity on a chosen parameter was then obtained by fixing other parameters at their reference values and changing the selected parameter within the limits given in Table 7. The upper limits were determined by considering the values given as

"super-advanced technology" by Wilcock et al. [23]. The results of reducing those parameters were also investigated, in order to observe the effect on engine performance when cooling techniques are negatively impacted during operations by conditions such as erosion, corrosion, sand/dust particles etc.

**Table 7. Cooling parameters used in the Sensitivity Analysis are shown with their reference values and percent change limits**

| Parameter | Reference Value | Change Limits |
|---|---|---|
| $Bi_m$ | 0.16 | ±12% |
| $Bi_{tbc}$ | 0.37 | ±53% |
| $\varepsilon_c$ | 0.75 | ±22% |
| $\varepsilon_{fc}$ | 0.4 | ±37.5% |
| $T_{b,max}$ | 1961 $^0$R | ±4% |

Sensitivity charts were then obtained for shaft power delivered, coolant flowrates (chargeable), and thermal efficiency by plotting the percent change in these parameters against the percent change in each selected cooling parameter of Table 7. In this type of analysis, the slope shows the comparative impact strength of various cooling parameters on the engine performance variables.

The thermal efficiency sensitivity is plotted in Figure 12. The sensitivity curves are not linear, due to changes in associated loss parameters when a cooling parameter is varied.

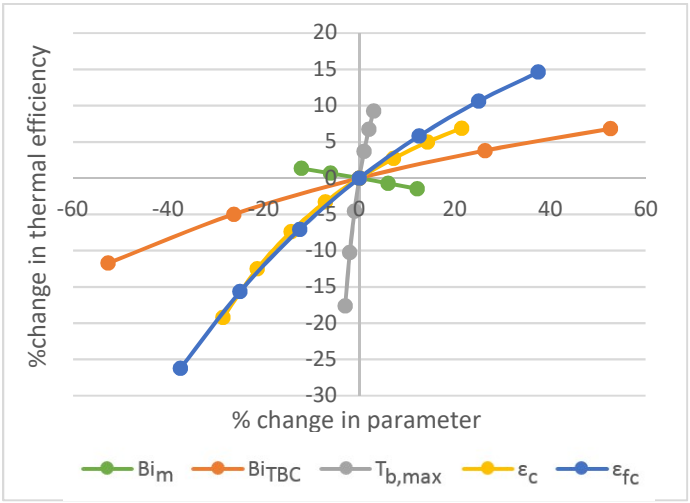


**Figure 12. Sensitivity of Thermal Efficiency of engine on selected cooling parameters**

In Figure 12, the slopes of sensitivity plots indicate that advancements in blade materials (through an increase in maximum allowable blade metal temperature, $T_{b,max}$) have the highest impact on the thermal efficiency, which is expected since it is the primary parameter that affects the overall blade cooling effectiveness. Advancements in film cooling techniques have the second highest impact followed by the advancements in internal cooling techniques and advancements in TBC materials. According to the heat transfer model used from Young et al. [7], if the blade material has a higher conductivity (thus a lower $Bi_m$) it can be cooled easier from the inside; resulting in a lower coolant flow requirement by external cooling techniques. Using less external coolant flow would eventually result in a decrease in turbine losses (mixing associated losses will be reduced) and the engine performance would be affected positively. It should be noted that this is valid only when advanced TBC materials and high film cooling effectiveness exist on the blade; with less advanced TBC technology and lower film cooling efficiency, cooling the blade metal internally might be compensated by the higher heat flux coming from the hot gas side.

Shaft power delivered is directly affected from increases in thermal efficiency of the gas turbine, and thus similar trends result, as shown in Figure 13.

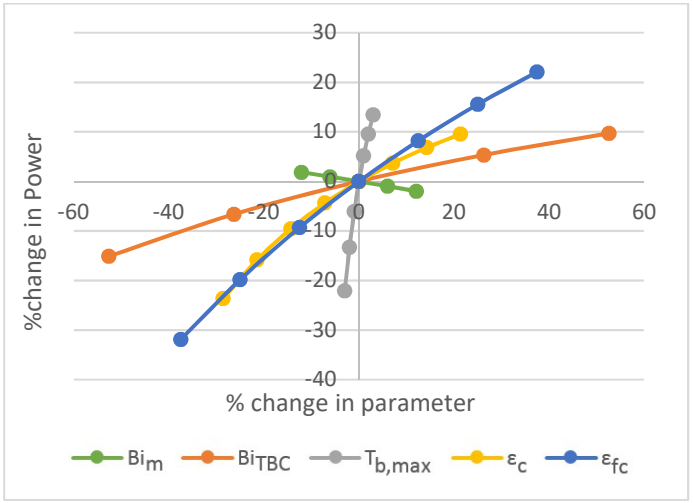


**Figure 13. Sensitivity of Shaft Power Delivered on selected cooling parameters**

As discussed, the sensitivities are directly dependent on how much a certain cooling technology is able to reduce the required coolant flowrates to cool the blade to the same maximum allowable temperature. Thus, the sensitivities of the coolant flowrates on considered cooling parameters are shown in Figure 14. Following the results on the other performance parameters, an increase in the maximum allowable blade temperature reduces the coolant requirement most, and this is followed by the advancements in film cooling techniques, internal cooling techniques and TBC materials, respectively. Due to the definition used for $Bi_m$, the slope has an opposite sign and the effect of using advanced blade materials should read in the opposite direction. Similar trends were obtained by Young et al. [7]; however, the numerical values of the slopes are different due to different values for cycle inputs.

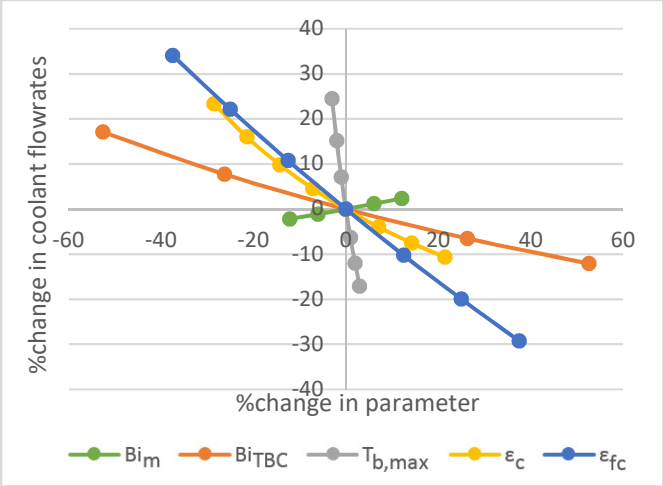


**Figure 14. Sensitivity of total coolant flowrates on selected cooling parameters**

The sensitivities obtained in this section also provide information about negative changes in cooling parameters as well. For instance, erosion of TBC material during operation might reduce the TBC thickness and reduce $Bi_{TBC}$. Sand or dust particles in the incoming airflow might fill the internal and external cooling channels, resulting in lower effectiveness values. Corrosion of the blade materials might change the maximum allowable blade metal temperature negatively. In such cases, the effects on the engine performance would be strongly influenced by changes in blade metal properties, then followed by negative effects on internal and external cooling channels and TBC erosion.

## 6. SUMMARY AND CONCLUSIONS

A cooled turbine model was developed using the model given by Young et al. [7] and was integrated into engine performance calculation models developed for high by-pass turbofan engines (CEDM) and industrial gas turbines (CGTM). Development of the CEDM was made from an earlier model developed for the same engine type [11] with changes in the usage of coolant flows in cycle calculations. This process also included defining the cooled engine case as an off-design point and modifying the related section accordingly. The CEDM, including the cooled turbine model, was then validated with GasTurb12 [13] and the effects of cooling the turbine on several engine parameters were analyzed. The effects of increasing turbine inlet temperature, by-pass ratio and flight Mach number show the expected trends for such engines.

An industrial gas turbine version of the model, CGTM was then developed from CEDM by including a methane combustion model, removal of components, and modification to cycle calculations as well as the mean-line turbomachinery design section. The CGTM was then validated with published available H-Class gas turbine data and GasTurb12. Validations made with turbine inlet temperature and ambient temperature show good agreement with referenced software and provided expected trends.

A sensitivity analysis using the CGTM was done with selected cooling technology parameters. The results of this analysis show that using a blade material that allows a higher maximum allowable blade temperature has the highest impact on increasing the gas turbine performance, followed by advancements in film cooling techniques (through increased adiabatic efficiency), advancements in internal cooling technologies and advancements in TBC materials.

When the blade material is fixed by structural design, following conclusions can be drawn from the sensitivity analysis:

- Although advancements in film cooling techniques provide the highest impact on increasing thermal efficiency, following this path only to increase engine thermal efficiency might require major changes in hole geometry, plenum and supply channel design
- Advancements in internal cooling techniques might also require major and costly design changes to internal cooling channel geometry and their configurations but internal cooling efficiency can also be increased by cooling of the coolant flow; which might be less expensive in development costs
- Although advancements in TBC materials show the lowest impact on increasing thermal efficiency, this path is also the easiest to achieve since only the coating needs to be changed and not the engine design.

It should be noted that the focus in this research was only to analyze the effects on the gas turbine performance; in the case of the sensitivity of a combined cycle performance on these parameters, the effect in the changes of exhaust temperature and pressure on other plant components would also need to be considered. The two models, CEDM and CGTM, have been validated and provide a valuable tool for turbine cooling, materials and durability researchers to take results from experimental and numerical design studies to determine the impact on overall engine performance of their designs, including cooling effectiveness, pressure drop and aerodynamic losses. The codes have been developed in-house at the Department of Energy, National Energy Technology Laboratory, and flowcharts of the algorithms will be made available to the turbine research and development community.

## NOMENCLATURE

| | |
|---|---|
| $\varepsilon$ | Cooling Effectiveness |
| $\pi$ | Exit to Inlet Total Pressure Ratio of the component |
| $\tau$ | Exit to Inlet Total Temperature Ratio of the component |
| $\eta$ | Isentropic Efficiency |
| Bi | Biot Number (hot gas side) |
| $f$ | Fuel-to-Air Ratio (at burner) |
| i | Cooled Turbine Stage Number |

| | |
|---|---|
| HR | Heat Rate |
| PSFC | Power Specific Fuel Consumption |
| TBC | Thermal Barrier Coating |
| TSFC | Thrust Specific Fuel Consumption |

*Subscripts*

| | |
|---|---|
| c | Compressor (single spool) |
| cH | High Pressure Compressor |
| cL | Low Pressure Compressor |
| g | Hot-gas |
| m | Metal |
| p | Propulsive Efficiency |
| rc | Coolant (rotor) |
| sc | Coolant (stator) |
| t | Turbine (single spool) |
| tH | High Pressure Turbine |
| th | Thermal Efficiency |
| tL | Low Pressure Turbine |
| tot | Total properties |

*Indexing of Engine Stations*

| | |
|---|---|
| 0 | Inlet |
| 1 | Diffuser Inlet |
| 2 | Low Pressure Compressor Inlet |
| 3 | High Pressure Compressor Inlet (Compressor Inlet in single spool) |
| 4 | Combustor Exit/Turbine Inlet |
| 4.1i | Cooled Turbine Purge Station before Stator |
| 4.2i | Cooled Turbine Stator Exit |
| 4.3i | Cooled Turbine Intermediate Purge Station/Rotor Inlet |
| 4.4 | High Pressure Turbine Exit (Turbine exit in single spool) |
| 4.5 | Low Pressure Turbine Inlet |
| 5 | Low Pressure Turbine Exit |
| 9 | Primary Exhaust Exit (Exhaust Exit in single spool) |
| 13 | Secondary Exhaust Exit |

*Indexing of Turbine Stations*

| | |
|---|---|
| p1 | Station after first purge injection |
| p2 | Station after second purge injection |
| r | Rotor exit |
| s | Stator exit |
| station,in | Inlet of the cooled turbine |
| station,ext | Exit of the cooled turbine |

## ACKNOWLEDGMENTS

This research was supported by an appointment to the National Energy Technology Laboratory Research Participation Program, sponsored by the U.S. Department of Energy and administered by the Oak Ridge Institute for Science and Education.

## REFERENCES

[1] Consonni S., (1992) “Performance Prediction of Gas/Steam Cycles for Power Generation”, PhD Dissertation to Princeton University, Center for Energy and Environmental Studies

[2] El-Marsi, M.A., (1988), “GASCAN- An Interactive Code for Thermal Analysis of Gas Turbine Systems”, *Journal of Engineering for Gas Turbines and Power*, Vol.110, pp.201-209

[3] Gauntner, J.W., (1980), “Algorithm for Turbine Cooling Flow and the Resulting Decrease in Turbine Efficiency”, NASA Technical Memorandum No.81453

[4] Lallini, V., Janikovic, J., Pilidis, P., Singh, R., and Laskaridis, P., (2012), “A Calculation Tool of a Turbine Cooling Air Schedule for General Gas Turbine Simulation Algorithms”, *Journal of Turbomachinery*, Vol.134, pp.041003/1-041003/8

[5] Li, Z, Zhao, L., Wang, B., Chi J., Zhang, S. and Xiao,Y., (2014), “A Thermodynamic Evaluation of GTCC/IGCC Based on a Quasi-One Dimensional Turbine Cooling Model”, *ASME GT2014-26534*

[6] Sanjay, O. S., and Prasad, B.N., (2008), “Comparative Performance Analysis of Cogeneration Gas Turbine Cycle for Different Blade Cooling Means”, *International Journal of Thermal Science*, Vol.48, pp.1432-1440

[7] Young J.B., and Wilcock R.C. (2002), “Modeling the Air-Cooled Gas Turbine: Part 2-Coolant Flows and Losses”, *ASME 2001-GT-392*

[8] Horlock, J.H., and Torbidoni, L., (2008), “Calculations of Cooled Turbine Efficiency”, *ASME GT2006-90424*

[9] Torbidoni, L. and Horlock, J.H., (2005), “A New Method to Calculate the Coolant Requirements of a High Temperature Gas Turbine Blade”, *Journal of Turbomachinery*, Vol. 127, pp.191-199

[10] Whitney, W., (1969), “Analytical Investigation of the Effect of Cooling Air on Two-Stage Turbine Performance”, NASA Technical Memorandum, NASA TM-X1728

[11] Uysal, S.C., (2014), “High By-Pass Turbofan Engines Aerothermodynamics Design and Optimization”, MSc. Thesis to

Middle East Technical University Department of Aerospace Engineering, Ankara, Turkey
[12] Mattingly Jack D. (2006), "Elements of Propulsion: Gas Turbines and Rockets / Jack D. Mattingly foreword by Hans von Ohain", American Institute of Aeronautics and Astronautics Inc., Reston, Virginia, USA
[13] GasTurb12 Software by GasTurb GmbH c/o Institute of Jet Propulsion and Turbomachinery Templergraben 55, 52062 Aachen, Germany
[14] Lufthansa Technical Training Manual ATA71-80 for A319/320/321 ENGINE CFM56-5A
[15] Esgar J.B., and Ziemer R.R., (1955), "Effects of Turbine Cooling with Compressor Air-Bleed on Gas Turbine Engine Performance", NACA Research Memorandum RM-E54L20
[16] Soares C., (2014) "Gas Turbines : A Handbook of Air, Land and Sea Applications (2nd Edition)". Jordan Hill, GBR: Elsevier Science & Technology
[17] Chappel, M.S., and Cockshutt,E.P. ,(1974), "Gas Turbine Cycle Calculations: Thermodynamic Data Tables for Air and Combustion Products for Three Systems of Units", National Research Council of Canada Division of Mechanical Engineering, Ottawa, ON
[18] National Institute of Technology (NIST), REFPROP Software using Standard Reference 23, Version 8.0
[19] GASEQ Software-Chemical Equilibria in Perfect Gases by Chris Morley, http://www.gaseq.co.uk
[20] Guha, A., (2001), "An Efficient Generic Method for Calculating the Properties of Combustion Products", *Proc. Instn. of Mech. Engrs.*, Vol.215, Part A, pp.375-387
[21] Giampaolo, T., (2003), "The Gas Turbine Handbook: Principles and Practices-2nd Ed.", The Fairmont Press Inc., Lilburn, GA
[22] Wilson, D.G., and Korakianitis T., (2014), "The Design of High Efficiency Turbomachinery and Gas Turbines-2nd Ed.", The MIT Press, Cambridge, MA
[23] Wilcock, R.C., Young, J.B., and Horlock, J.H., (2005), "The Effect of Turbine Blade Cooling on the Cycle Efficiency of Gas Turbine Power Cycles", Journal of Engineering for Gas Turbines and Power, Vol.127, pp.109-120
[24] Gas Turbine World, "2015 Performance Specs", 31st Edition, January-February 2015, Volume 45, No.1, Pequot Publishing Inc.

## APPENDIX-A

## INPUTS OF COOLED ENGINE MODELS

Cooled Engine Model Input list is given in Table-A1 with the values used for case-specific test validations with a turbofan engine, Cooled Gas Turbine Model Input list is given in Table-A2 with the values used for case specific test validations with a generic H-Class engine scenario.

**Table A 1 CEDM Cycle and Cooling Inputs used in validations**

| *Name of the Parameter* | *Value of the Parameter* |
|---|---|
| ***Flight Mach Number ($M_0$)*** | 0.8 |
| ***Flight Altitude [ft]*** | 33000 |
| ***Engine Mass Flow Rate ($\dot{m}_0$) [lbm/s]*** | 938.9 |
| ***By-Pass Ratio ($\alpha$)*** | 6 |
| ***Bleed Air Fraction ($\beta$) [%]*** | 3.0 |
| ***Fan Pressure Ratio ($\pi_f$)*** | 1.55 |
| ***Low Pressure Compressor Pressure Ratio ($\pi_{cL}$)*** | 1.55 |
| ***High Pressure Compressor Pressure Ratio ($\pi_{cH}$)*** | 17.1 |
| ***Diffuser Pressure Ratio ($\pi_d$)*** | 0.99 |
| ***Combustor Pressure Ratio ($\pi_b$)*** | 0.95 |
| ***Nozzle Pressure Ratio ($\pi_n$)*** | 0.99 |
| ***Fan Nozzle Pressure Ratio ($\pi_{nf}$)*** | 0.99 |
| ***Combustor Efficiency ($\eta_b$)*** | 0.99 |
| ***High Pressure Spool Mechanical Efficiency ($\eta_{mH}$)*** | 0.99 |
| ***Low Pressure Spool Mechanical Efficiency ($\eta_{mL}$)*** | 0.99 |
| ***High Pressure Spool Power Takeoff Efficiency ($\eta_{mPH}$)*** | 0.99 |
| ***Low Pressure Spool Power Takeoff Efficiency ($\eta_{mPL}$)*** | 1.0 |
| ***Fan Polytropic Efficiency ($e_f$)*** | 0.93 |
| ***Low Pressure Compressor Polytropic Efficiency ($e_{cL}$)*** | 0.91 |
| ***High Pressure Compressor Polytropic Efficiency ($e_{cH}$)*** | 0.91 |
| ***High Pressure Turbine Polytropic Efficiency ($e_{tH}$)*** | 0.93 |
| ***Low Pressure Turbine Polytropic Efficiency ($e_{tL}$)*** | 0.93 |
| ***Fuel Heating Value ($h_{PR}$) [Btu/lbm]*** | 18400 |
| ***High Pressure Turbine Inlet Temperature ($T_{t4}$) [$^0$R]*** | 2768.7 |
| *Cooling Inputs* | |
| ***$Bi_m$*** | 0.16 |
| ***$Bi_{tbc}$*** | 0.35 |
| ***$\eta_c$*** | 0.7 |
| ***$\eta_{fc}$*** | 0.4 |
| ***$T_{b,max}$*** | 1961 $^0$R |
| ***Purge Fraction (%of mainstream)*** | 0.1 |
| ***Cooling Configuration*** | [Internal+Film+TBC] |
| ***Film Cooling Effective Injection Angle (deg)*** | 30 |

**Table A 2 CGTM Cycle and Cooling Inputs used in validations**

| *Name of the Parameter* | *Value of the Parameter* |
|---|---|
| ***Ambient Pressure (psia)*** | 14.696 |
| ***Ambient Temperature [$^0$R]*** | 529.67 |
| ***Engine Mass Flow Rate ($\dot{m}_0$) [lbm/s]*** | 1433 |
| ***Compressor Pressure Ratio ($\pi_{cH}$)*** | 21.5 |
| ***Diffuser Pressure Ratio ($\pi_d$)*** | 0.99 |
| ***Combustor Pressure Ratio ($\pi_b$)*** | 0.97 |
| ***Nozzle Pressure Ratio ($\pi_n$)*** | 0.95 |
| ***Combustor Efficiency ($\eta_b$)*** | 0.98 |
| ***Shaft Mechanical Efficiency ($\eta_{mH}$)*** | 0.995 |
| ***Generator Efficiency ($\eta_{gen}$)*** | 0.99 |
| ***Compressor Polytropic Efficiency ($e_{cH}$)*** | 0.89 |
| ***Turbine Polytropic Efficiency ($e_{tH}$)*** | 0.9 |
| ***Fuel Heating Value ($h_{PR}$) [Btu/lbm]*** | 21397.2 |
| ***High Pressure Turbine Inlet Temperature ($T_{t4}$) [$^0$R]*** | 3232 |
| *Cooling Inputs* | |
| ***$Bi_m$*** | 0.15 |
| ***$Bi_{tbc}$*** | 0.35 |
| ***$\eta_c$*** | 0.7 |
| ***$\eta_{fc}$*** | 0.4 |
| ***$T_{b,max}$*** | 2008 $^0$R |
| ***Purge Fraction (%of mainstream)*** | 0.5 |
| ***Cooling Configuration*** | [Internal+Film+TBC; Internal+Film+TBC; Internal+TBC; Internal Only] |

## APPENDIX-B

## VALIDATION OF METHANE COMBUSTION PROPERTY DATA

Methane combustion properties, generated with REFPROP and GASEQ Software was validated with the methane combustion enthalpy data given by Guha [20] with the low and high temperature range temperature difference scenarios given in Table-B. The sub-system that calculates the thermodynamic properties in CGTM was named as 'F-AIRng', and denoted with this name in the tables.

**Table B Methane combustion properties were validated with the enthalpy scenarios for 5 different fuel-to-air ratios (*f*) given by Guha [20]**

| *Low Temperature Test ($T_1$=1080 $^0$R, $T_2$=1800 $^0$R)* | *Δh (F-AIRng)* | *Δh [20]* | *%Difference* |
|---|---|---|---|
| *f=0.01* | 0.452 MJ | 0.450 MJ | 0.44% |
| *f=0.02* | 0.464 MJ | 0.461 MJ | 0.65% |
| *f=0.03* | 0.474 MJ | 0.471 MJ | 0.64% |
| *f=0.04* | 0.485 MJ | 0.481 MJ | 0.83% |
| *f=0.05* | 0.495 MJ | 0.491 MJ | 0.81% |
| *High Temperature Test ($T_1$=2160 $^0$R, $T_2$=3600 $^0$R)* | *Δh (F-AIRng)* | *Δh [20]* | *%Difference* |
| *f=0.01* | 1.009 MJ | 1.005 MJ | 0.40% |
| *f=0.02* | 1.042 MJ | 1.034 MJ | 0.77% |
| *f=0.03* | 1.072 MJ | 1.063 MJ | 0.84% |
| *f=0.04* | 1.100 MJ | 1.092 MJ | 0.73% |
| *f=0.05* | 1.128 MJ | 1.117 MJ | 0.98% |